High-speed Three-dimensional Shape Measurement Using Spatial Frequency Encoding and DLP Projector

Yanshuai Tu, Yong Li*, Hongzhen Jin and Jian Wang
Institute of Information Optics, Zhejiang Normal University, Jinhua, China

ABSTRACT

A method for high-speed three-dimensional measurement with low-speed camera is proposed. The spatial frequency encoded fringes are projected with high frame rate and deformed fringes are captured with low frame rate. Several fringes are integrated in one captured image. The directions and/or frequencies of these fringes are different. The spatial frequency spectrum of these fringes is separate in spatial frequency domain. So, the phases of different fringes can be obtained by filtering the image with different filters. Then several 3D shapes of different time are obtained from one captured image. The experiments are carried out to verify proposed method and measurement results are demonstrated. The method improves the speed of 3D shape measurement and reduces the cost of measurement system as well.

Keywords: 3D shape measurement, spatial frequency encoding, Fourier transform profilometry, DLP projector

1. INTRODUCTION

Fringe projection is a general technique for acquiring three-dimensional (3D) surface information. Based on fringe projection, several methods have been exhaustively studied including Moiré technology(MT)[1,2], phase measuring profilometry(PMP)[3,4], Fourier transformation profilometry(FTP)[5,6] and spatial phase detection(SPD)[7-9]. Among them, some methods always require multi-fringe to derive shape information, e.g. PMP requires at least three phase shift fringes to decode the modulated phase. Others require just one fringe.

High speed 3-D shape measurement can be applied to industry detection, facial expression recording and dynamic procedure recording. FTP which requires only one fringe to be projected is a popular one in high speed 3D measurement. FTP measurement involves three steps: (1) projecting a grating onto object, (2) recording the deformed fringe pattern by a camera, and (3) processing the images to acquire the 3D surface information. A digital projector is usually applied in the step of projecting due to its flexibility. The FTP method has been extensively researched in precise and height variation. Among them, the frequency-multiplex technology [10] permits the 3D shape measurement of objects with discontinue height step and/or spatially isolated surfaces. Scheme of π phase shifting extend the slope of height variation to nearly three times that of the unimproved FTP [11].

It is possible to acquire high speed 3-D shape if frame rate of camera is fast enough. High-speed cameras employ communication protocols such as IEEE 1394, USB3.0, Giga Ethernet and Camera Link. Special hardware is used in the communication to achieve bandwidth from 0.8Gbps to 5.4Gbps. However, high speed cameras are expensive and the transmission rate is invariably limited. On the other hand, projector based on digital-light-processing (DLP), can work at thousands frames per second, and the cost is relatively low. Many high speed 3D measurement systems have token the advantages of DLP projectors to achieve a rapid projection of fringes [12]. In the situation of using DLP to project fringes, the obstacle to higher speed 3D measurement is the transmission burden of camera.

The purpose of this contribution is to increase the speed of 3D shape measurement by depressing camera transmission bandwidth, using the advantages of DLP projector. The main idea is to project fringes rapidly and capture one superposed deformed fringe. And multiple 3D shapes of different time are derived from the superposed image. The projected fringes are frequency and/or direction different. It means that the deformed fringes are encoded with different spatial frequencies. Due to the property of fringe projection we will show later, the spatial spectrum of captured superposed image is separate and each spatial spectrum of each time can be obtained by filtering properly. The inverse Fourier transform is applied to each spatial spectrum island and the phases in different time can be obtained.

*E-mail: liyong@zjnu.cn, Telephone: 86 (0)579 82298863

The structure of this paper is as follows. Section 2 introduces the principle of our method. Section 3 discusses how DLP technology can be used and the issues related to synchronization of the camera and the projector. Experiments are carried out. Conclusion is drawn in Sec. 4.

2. PRINCIPLE

2.1 FTP principle

The general geometry of fringe projection system is shown in Fig. 2.1. C_1C_2 is the optical axis of a camera. The optical axis of projector is P_1P_2. O is the cross point of camera and project optical axis on reference plane R. D is a point on the object surface with height h to reference plane. L_0 is the distance between C_2 and O.

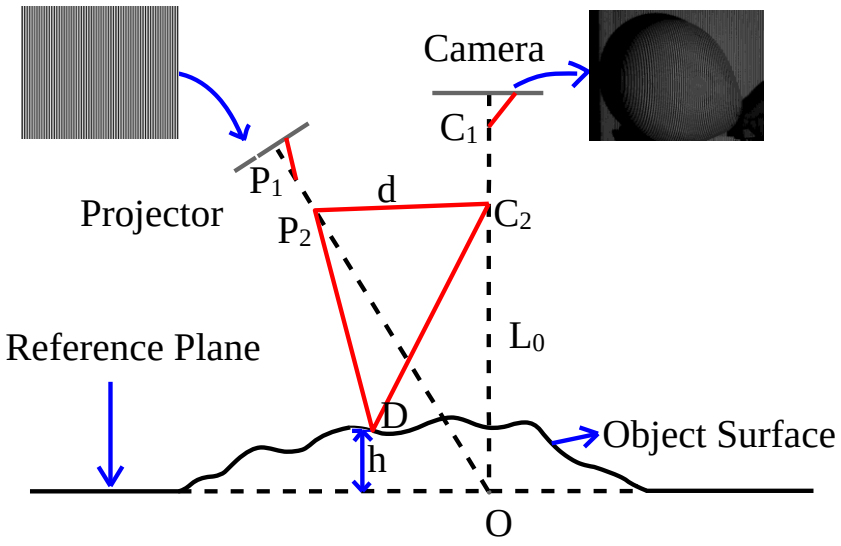

Fig. 2.1 Optical geometry of fringe projection system

If a sinusoidal grating is projected, the deformed fringe captured by a camera can be expressed as

$$g(x,y) = a(x,y) + b(x,y)\cos(2\pi f_0 x + \phi(x,y)) \tag{1.1}$$

where, $a(x,y)$ is background illumination, $b(x,y)$ is the intensity modulation and $\phi(x,y)$ is the additional phase caused by object height distribution. f_0 is the fundamental frequency of captured image.

The spectrum of $g(x,y)$ can be expressed as

$$G(f) = \mathcal{F}\{a(x,y)\} + \mathcal{F}\{\frac{1}{2}b\exp(i\phi)\} * \delta(f - f_0) + \mathcal{F}\{\frac{1}{2}b\exp(-i\phi)\} * \delta(f + f_0) \tag{1.2}$$

where, $\mathcal{F}$ is the Fourier transform operator, * is the convolution operator.

$G(f)$ consists of three part as shown in Fig 2.2. The first one is the spectrum of $a(x,y)$. The second part is $Q_2 = \mathcal{F}\{\frac{1}{2}b\exp(i\phi)\} * \delta(f - f_0)$ and the third part is $Q_3 = \mathcal{F}\{\frac{1}{2}b\exp(-i\phi)\} * \delta(f + f_0)$. In most cases, $a(x,y)$, $b(x,y)$ and $\phi(x,y)$ vary slowly compare with projected fringe. It means each part of $G(f)$ have no high frequency components. If $f_b < f_{1\min}$, where f_b is maximal frequency of zero order component, $f_{1\max}$, $f_{1\min}$ are maximal and minimal frequency of fundamental component, then the three items of $G(f)$ is isolate.

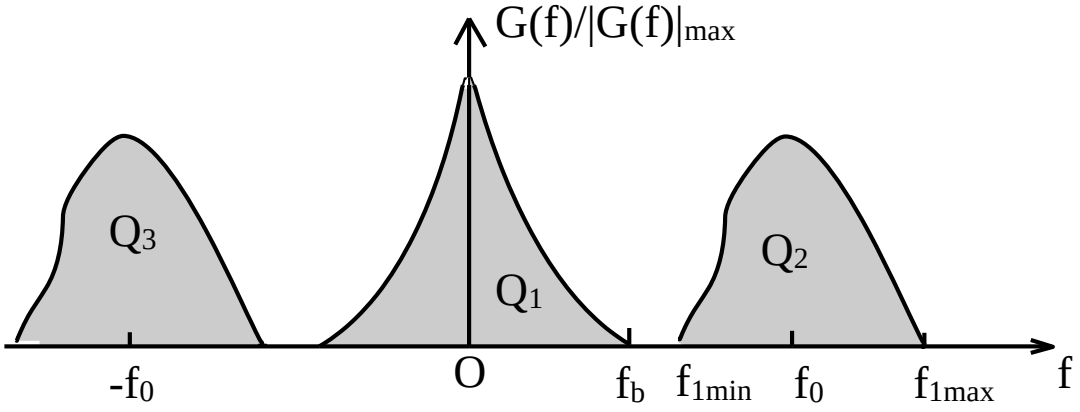

Fig. 2.2 Spectrum of deformed fringe

If the second part is kept and apply inverse Fourier transform to it, the signal can be expressed as

$$\hat{g}(x,y) = Ab(x,y)\exp\left(i(2\pi f_0 x + \phi(x,y))\right). \tag{1.3}$$

similarly, on the reference plane R, the deformed fringe image is written by

$$\hat{g}_0(x,y) = Ab_0(x,y)\exp\left(i(2\pi f_0 x + \phi_0(x,y))\right), \tag{1.4}$$

where $b_0(x,y)$ is the intensity modulation of reference plane. $\phi_0(x,y)$ is the phase modulated by reference plane. Equ. (1.3) multiply conjugate complex of Equ. (1.4), following formula can be obtained

$$\Delta\psi(x,y) = \mathrm{Im}\{\log(\hat{g}\hat{g}_0^*)\} \tag{1.5}$$

The phase $\Delta\psi(x,y)$ derived from Equ. (1.5) is the wrapped phase of $\Delta\phi(x,y) = \phi(x,y) - \phi_0(x,y)$ and gives principal values ranging from $-\pi$ to π. Continuous phase can be obtained by phase unwrapping algorithm. Then the height distribution can be computed by the following formula, if $L_0,\ d$ is given:

$$h(x,y) = \frac{L_0\Delta\phi(x,y)}{\Delta\phi(x,y) - 2\pi f_0 d},$$

(2.1.6)where $\Delta\phi(x,y)$ is the unwrapped phase of $\Delta\psi(x,y)$.

2.2 Spatial Frequency Encoding Scheme

In this part, we firstly express FTP using a more general fringe, and discuss the encode phenomena of phase in the view of frequency spectrum. Secondly, we discuss the principle of Spatial Frequency Encoding. And then, Spatial Frequency Encoding Scheme (SFE) is outlined.

If a more general fringe projects onto the object, the fringe can be expressed as

$$I = 1 + \cos(2\pi f_x x + 2\pi f_y y), \tag{1.7}$$

where f_x, f_y are the frequencies of x, $y$directions of a fringe, respectively. It means fringe vary not only in x direction, but also in y direction. The fringe is same to the case in Section 2.1 when $f_y = 0$. Here, denote $C = (f_x, f_y)$ to the 2D frequency of the fringe.

Now, the deformed fringe of captured image can be expressed as

$$g(x,y) = a(x,y) + b(x,y)\exp(i(2\pi f_x x + 2\pi f_y y + \phi(x,y))), \tag{2.1.8}$$

Compared with one dimensional fringe, two dimensional Fourier transform should be adopted. Similar to one dimensional fringe, the spectrum is isolate too. Each separate area is called a spectrum island.

When the captured image is filtered with a 2D band pass spatial filter around spectrum island center $C = (f_x, f_y)$, the output can be expressed as

$$\hat{g}(x,y) \propto \exp\left(i(2\pi f_x \cdot x + 2\pi f_y \cdot y + \phi(x,y))\right). \tag{2.1.9}$$

When projecting a fringe with $C = (f_x, f_y)$, the phase modulated by height are encoded into spectrum island at center $C = (f_x, f_y)$. At different time, project different fringe with different frequency$C_t = (f_{tx}, f_{ty})$, then each $\phi_t(x,y)$

is encoded by different center and form different spectrum island. Since the center of fringe is intended separate enough, the frequency domain is still separated when multiple phase information are encoded into a same spectrum. That is to say, if a superposed image of different fringe projecting at different time is recorded, we can obtain each fringe and then recover each phase.

To be specific, as shown in Fig. 2.4, the proposed scheme is demonstrated under the condition of N=3. First, we project fringe i at time i for i=1, 2, 3. During the period of projection, a superposed image Ds is recorded. Ds is the sum up of $D1$, $D2$ and $D3$ since the exposure of CCD is linear superposition. Ds Can be expressed as

$$\mathrm{Ds}(x,y) = \sum_{t=1}^{3}\{a(x,y) + b_t(x,y)\exp(i(2\pi f_{tx}x + 2\pi f_{ty}y + \phi_t(x,y)))\}. \quad (2.1.10)$$

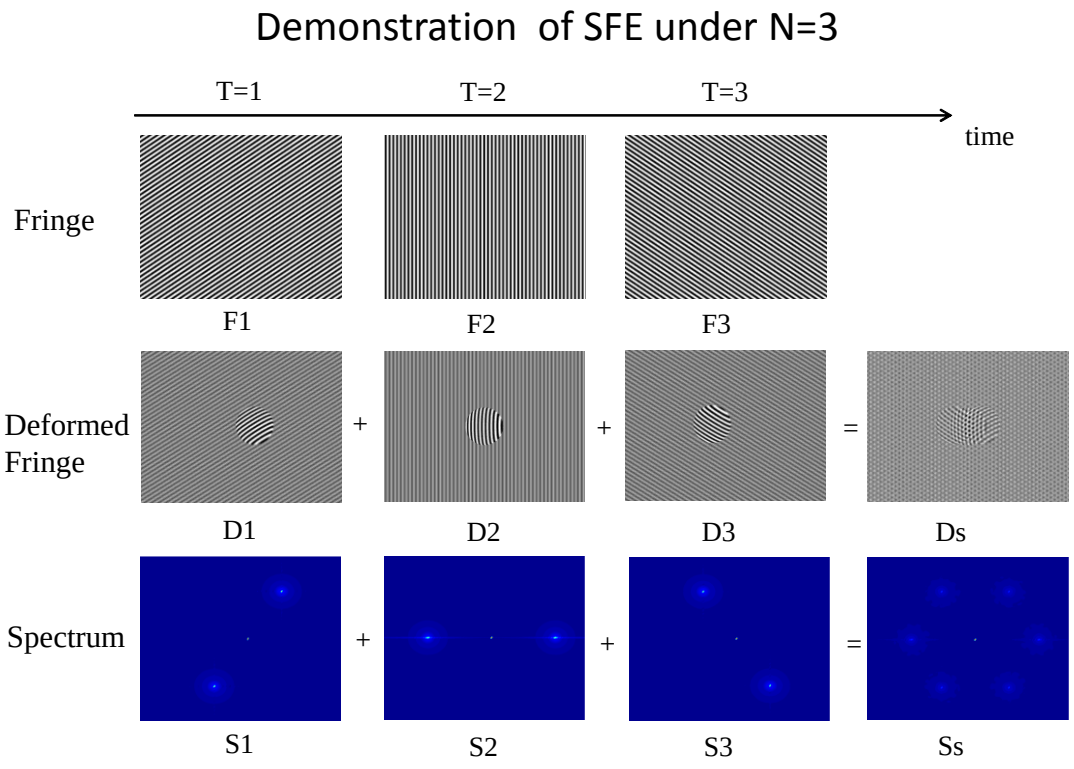

Fig. 2.4 demo of SFE under N=3

Ss is the spectrum of Ds, which is sparse and separate as shown in Fig. 2.4. By selecting a filter on Ss, we can obtain complex signal for any given t,

$$\hat{g}_t(x,y) \propto \exp\left(i(2\pi f_{tx}\cdot x + 2\pi f_{ty}\cdot y + \phi_t(x,y))\right). \quad (1.11)$$

Similarly, phase difference information can be calculated as,

$$\Delta\psi_t(x,y) = \mathrm{Im}\{\log\left(\hat{g}_t\hat{g}_0^*\right)\}. \quad (2.1.12)$$

Second, filter and recover phase for t=1, 2, 3, we can totally obtain 3 phase information. Each phase contains height distribution at different time. Finally, repeat steps one and two, to record a sequence of motion and derive the 3D information during the whole time.

The accuracy of proposed scheme is depending on the precise of complex signal $\hat{g}_t(x,y)$. The measurement limitation of SFE is discussed here. The locally spatial frequency is define as

$$f_t(x,y) = C_t + \nabla\phi_t \quad (1.13)$$

where C_t is the two dimensional carrier frequencies and ∇ is the gradient operator $\nabla = \frac{\partial}{\partial x}\vec{i} + \frac{\partial}{\partial y}\vec{j}$. To avoid frequency aliasing, islands should be separated from each other. That is to say, below equations exits

$$|\nabla\phi_t|_{\max} + |\nabla\phi_i|_{\max} < 2\pi|C_tC_i|, i \neq t; i, t = 1, 2, ...N. \tag{1.14}$$

$$|\nabla\phi_t|_{\max} + |\nabla a(x, y)|_{\max} < 2\pi|C_t|. t = 1, 2, ...N. \tag{1.15}$$

Equ. (1.14) constrain spectrum islands are separate from each other. Equ. (1.15) constrain spectrum islands depart with the spectrum of background illumination.

In most cases, the situations are satisfied. Firstly, the proposed method is under the constrain that $a(x, y)$ and $\phi(x, y)$ change slowly that made themselves isolated a small area around the fringe center in spectrum. Secondly, the phase information $\phi(x, y)$ varies around the frequency of fringe and fringes are designed to be separate. If one of the above conditions become invalid, the phase information will mix each other and leading out inaccurate height.

3. EXPERIMENT AND RESULTS

3.1 Synchronization of device

The proposed method requires camera expose during each projection period. So, the synchronization of camera and projector is a key point. High frame rate projection can be achieved by DLP projector. The image of DLP projector is created by digital micro-mirror device (DMD). A DMD is consists of millions of micro mirrors which operate in a very high-speed bi-stable mode up to 20,000 rotation in a second. Binary image depresses the transition bandwidth and makes projector work at high frame rate. The synchronization scheme is serving to the proposed method as shown in Fig. 3.1. The projector generates a vertical sync when a frame is finished and preparing to project another image. This signal is detected by a FPGA and then it triggers the camera when N frames of fringes are projected onto the object. At the same time, the FPGA also generate the project fringe signal. In theory, the camera exposure time is exactly equal to the projection period of N fringes. However, there is a little time delay between the trigger signal and camera exposure start time point. So the exposure time of camera shall be slightly less than the time of N fringes projection.

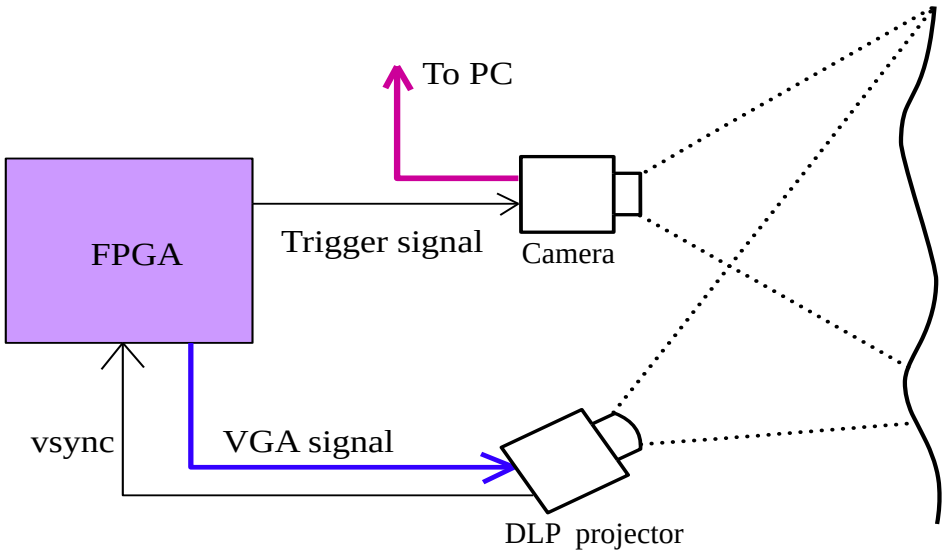

Fig. 3.1 Synchronization Scheme

Experiments are conducted under the condition of N=3. In this case, a DLP projector fringes at 360fps the resolution of 1024x768 and camera capture images at 120fps under the resolution of 640x480. Since the DLP projector can divide a VGA signal into R, G, B in time sequence. So the VGA image is actually a composite image of three fringes. In the experimental setup, the three fringes are designed with three different angles, and horizontal period of fringe is 20 pixels.

3.2 Experimental results

First, we measured a damping pendulum on a plane. The physical device is shown as Fig. 3.2a. Pendulum is fixed to point *P* and oscillates on the x-O-y plane. Reference plane is set at Z=0. Fig. 3.2b is one of captured image. The 2D

spectrum of the superposed image is shown in Fig. 3.2c. Obviously, the spectrum islands are separate. The corresponding filter is drawn by circles in Fig. 3.2c. The first phase distribution is shown in Fig. 3.2d.

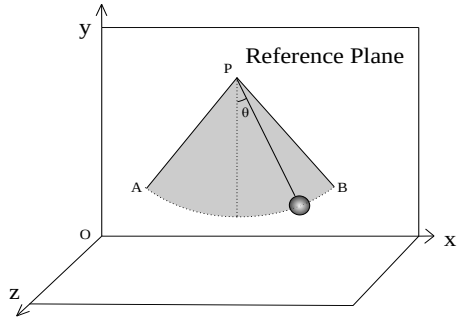

a. Pendulum

b. A superposed deformed image

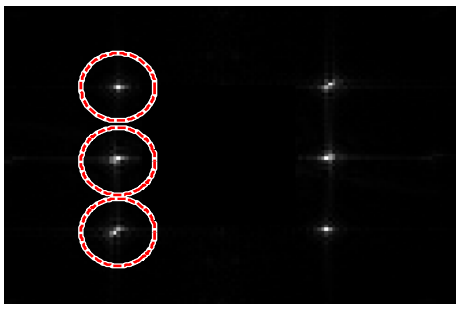

c. Spectrum and filters

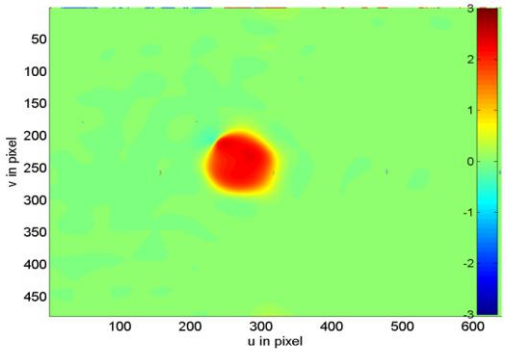

d. First phase distribution

Fig. 3.2 3D measurement of a Pendulum

All the motion of pendulum is captured and recovered. The center of the pendulum, i.e. the location of maximal value of phase, is shown in time serial in Fig. 3.3.

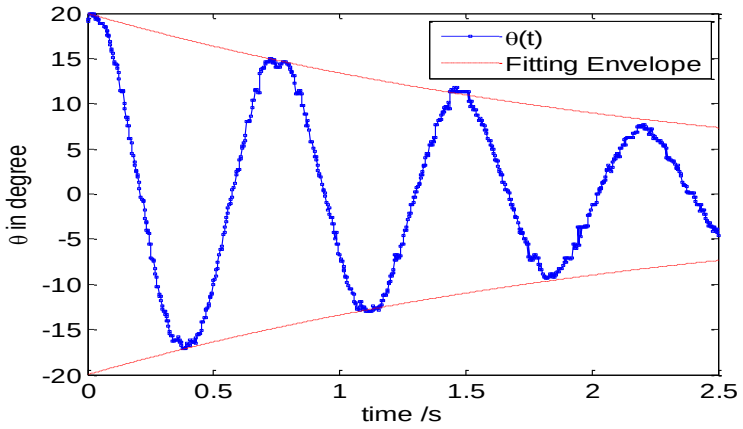

Fig. 3.3 Observation of $\theta(t)$

In Fig. 3.3, the dot line is oscillator angle in time. We can find the vibration energy is reduction since it is a damped system. The fitting envelop is a fitting line with the form of $\pm A\exp(-\beta t)$. The envelop line fit the observation angle well, it says the phase measurement is accurate.

The same equipment is also used to measure a fast changing facial expression. The selected results are shown in Fig. 3.4. Each frame of Fig. 3.4 is a recovered phase at different time. The expression is from serious to smile. At time t=0, the eyes are closed and perform a serious countenance. With time elapse, smile begins.

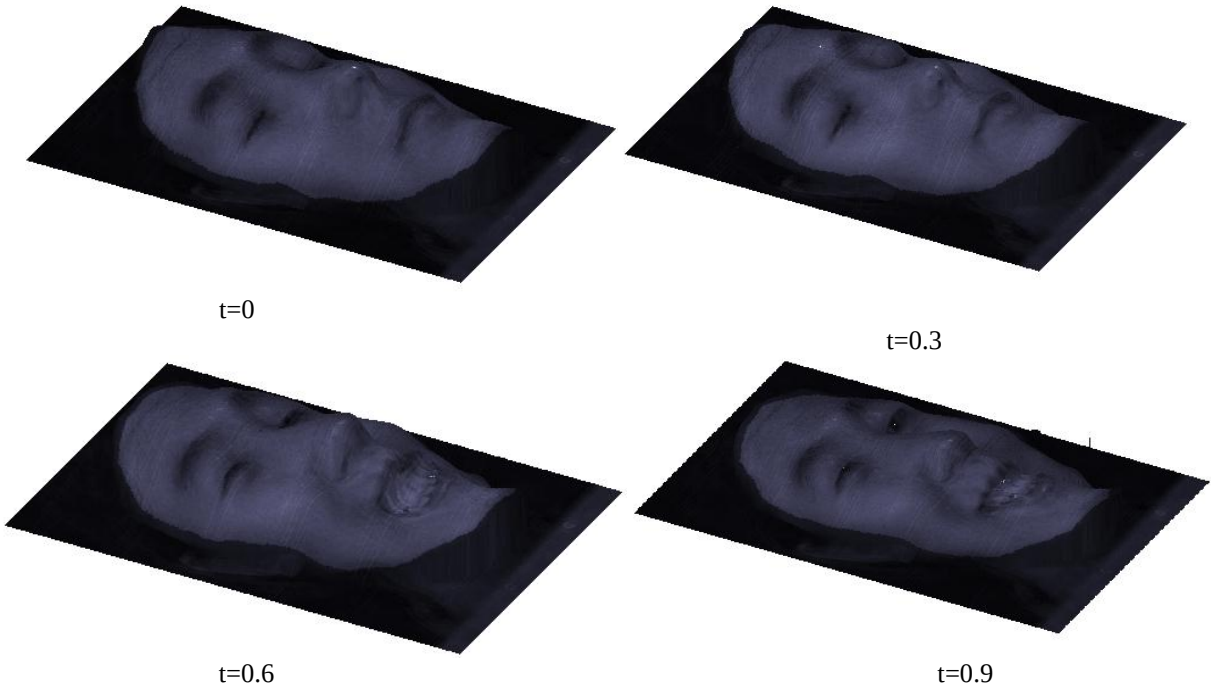

Fig. 3.4 Selected experimental results of facial expression change

4. CONCLUSION

In this paper, a spatial frequency encoding scheme is presented to acquire high-speed dynamic three-dimensional information with low-speed camera and DLP projector. The time information is encoded with spatial frequency of fringe pattern. Multiple deformed fringes are exposed into one image and deformed fringe information at each time is recovered by spectrum filtering. The experimental results reveal that this method is valid. The data transition rate is depressed and the speed of 3D shape measurement is improved. The cost of measurement system is reduced as well.

REFERENCES

[1] D. M. Meadows, W. O. Johnson, and J. B. Allen, "Generation of surface contours by moir épatterns," Appl. Opt. 9, 942-947 (1970).
[2] T. Yoshizawa, "The recent trend of moir émetrology," Journal of Robotics and Mechatronics 3(3), 157-162 (1991).
[3] V. Srinivasan, H. C. Liu, and M. Halioua, "Automated phase-measuring profilometry of 3-d diffuse objects," Appl. Opt. 23, 3105-3108 (1984).
[4] X.-Y. Su, W.-S. Zhou, G. von Bally, and D. Vukicevic, "Automated phase-measuring profilometry using defocused projection of a Ronchi grating," Optics Communications 94(6), 561-573 (1992).
[5] M. Takeda and K. Mutoh, "Fourier transform profilometry for the automatic measurement of 3-d object shapes," Appl. Opt. 22, 3977-3982, (1983).
[6] X. Su and W. Chen, "Fourier transform profilometry:: a review," Optics and Lasers in Engineering 35(5), 263-284 (2001).
[7] S. Toyooka and Y. Iwaasa, "Automatic profilometry of 3-d diffuse objects by spatial phase detection," Appl. Opt. 25, 1630-1633 (1986).
[8] M. Sajan, C. Tay, H. Shang, and A. Asundi, "TDI imaging tool for profilometry and automated visual inspection," Optics and Lasers in Engineering 29(6), 403-411 (1998).
[9] M. Sajan, C. Tay, H. Shang, and A. Asundi, “Improved spatial phase detection for profilometry using a TDI imager," Optics Communications 150(1), 66-70 (1998).

[10] M. Takeda, Q. Gu, M. Kinoshita, H. Takai, and Y. Takahashi, "Frequency-multiplex Fourier-transform profilometry: a single-shot three-dimensional shape measurement of objects with large height discontinuities and/or surface isolations," Appl. Opt. 36, 5347-5354 (1997).
[11] X. Mao, W. Chen, and X. Su, "Improved Fourier-transform profilometry," Appl. Opt. 46, 664-668 (2007).
[12] T. Bell and S. Zhang, "Toward superfast three-dimensional optical metrology with digital micro mirror device platforms," Optical Engineering 53(11), 112-206 (2014).